

Portable multi-spectral lens-less microscope with wavelength-self-calibrating imaging sensor

Yinxu Bian^{a,b,1}, Qulan Liu^{a,b,1}, Zhifeng Zhang^{a,b,c}, Dyi Liu^{a,b}, Anwar Hussain^{a,b,e}, Cufang Kuang^{a,b,d,*}, Haifeng Li^{a,b,*}, Xu Liu^{a,b,d}

^a State Key Laboratory of Modern Optical Instrumentation, Zhejiang University, Hangzhou 310027, China

^b College of Optical Science and Engineering, Zhejiang University, Hangzhou 310027, China

^c School of Physics and Electronic Engineering, Zhengzhou University of Light Industry, Zhengzhou 450000, China

^d Collaborative Innovation Center of Extreme Optics, Shanxi University, Taiyuan 030006, China

^e Quantum Optics Lab, Department of Physics, COMSATS Institute of Information Technology, Islamabad, Pakistan



ARTICLE INFO

Keywords:

Microscopy
Digital holography
Phase retrieval
Computational imaging
Portable imaging device

ABSTRACT

Multi-spectral imaging technology is helpful to obtain better contrast and more details of images at different wavelengths compared with monochromatic imaging or conventional RGB imaging technologies. And in resource-limited areas, microscopes with features of low-cost and portability are extremely attractive. In this manuscript, we demonstrate that cost-effective lens-less microscopy can be combined with the multi-spectral imaging technology, which can be alternative to conventional approaches and applied in biology, chemistry, environmental science. As a proof of this concept, we present a novel portable multi-spectral lens-less microscope (MSLLM). An outstanding highlight of our setup is its wavelength-self-calibrating imaging sensor (WSCIS), which can provide computationally optimized wavelength value (COWV) for LED illumination in real time. For each illumination, 5 holograms of the sample at 5 different heights are captured. Through the COWVs and phase retrieval algorithms, 7 multi-spectral images (FOV: 4.8 mm × 4.6 mm, resolution: ~1 μm) can be reconstructed. We believe that our MSLLM can be widely applied to multi-spectral microscopy in low-cost required scenes.

1. Introduction

Optical imaging technologies have been used in biology, medical science and material science for centuries because of their non-invasive analysis and measurement. Especially, microscopic techniques combined with other optical technologies, such as OCT microscopy, hyperspectral microscopy, interference microscopy, and so on, help a lot to observe micro-structures and micro-activities. This manuscript discussed is about a lens-less microscopy combined with multi-spectral imaging. Usually, a spectral imager [1–7] records images at several illuminating wavelengths accordingly. These data cubes are very helpful to get better contrast and details of images at different wavelengths, which may be further useful in identifying the composition and structure of objects. Most spectral imagers require the sophisticated temporal scanning configuration to obtain a multi-spectral image data cube. For example, a dispersive push-broom slit spectrometer [1,2] measures the spectrum at each point in the scene that is imaged onto a slit and relies on the spatial motion of either the slit or the object to measure the complete data cube. The spectral resolution is dependent on the dispersive opti-

cal elements, such as prisms and gratings. A spectrally filtered imager [3] takes multiple images of the same scene consecutively with different discrete wavelength filters, and its spectral resolution is the bandwidth of spectral filter. A Fourier-transform spectral imager [4,5] requires the scanning of the optical path difference between two arms of a Michelson interferometer. The above mentioned spectral imagers are precisely scientific tools to measure and analyze targets noninvasively. And all of them can be combined with conventional microscopes to further analyze the micro-world.

However, in resource-limited cases, especially in fields and remote areas, compact and cost-effective devices are more attractive. Many portable microscopes are developed [8–20]. A cost-effective fluorescence mini-microscope is applied in biomedical science, with adjustable magnifications 8X–60X and a resolution ~2 μm, using a USB web camera with a flipped lens. [8] Cost-effective microscopes based on cellphones are also developed [10–13]. Besides the above lens-based portable microscopes, lens-less microscopes are developed [14–20]. They all can be assembled with multi-spectral imaging technologies, but in contrast to lens-based portable microscopes, lens-less microscopes may have a

* Corresponding authors.

E-mail addresses: cukuang@zju.edu.cn (C. Kuang), lihaifeng@zju.edu.cn (H. Li).

¹ These authors contributed equally in this work.

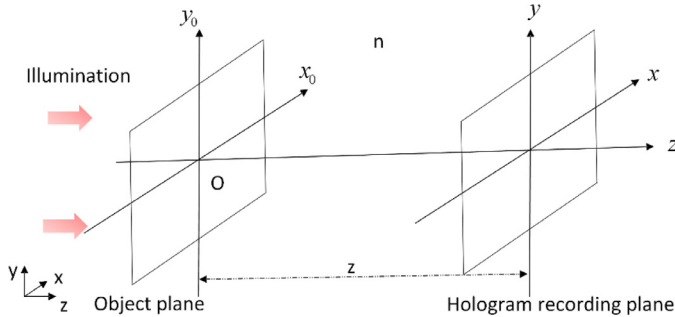


Fig. 1. Schematic of scalar wave propagation theorem.

better resolution theoretically. Main reasons are as follows: In a lens-based system, NA and aberrations limit the resolution. For aberrations-corrected optical system, the resolution is limited by the Rayleigh criterion ($\sigma = 0.61\lambda/\text{NA}$, where σ is the spot size and λ is the illumination wavelength) [21]. Usually in a portable lens-based microscope, NA is less than 0.2. But in lens-less microscopes, the optical wave propagates in free space, so the NA can be viewed as a value close to 1.

In this manuscript, we demonstrate that low-cost lens-less microscopy can be combined with the multi-spectral imaging technology. To testify this concept, we present a novel low-cost portable multi-spectral lens-less microscope (MSLLM) with multi-LEDs illumination. The aim is to promote multi-spectral lens-less imaging analysis in some special scenes, e.g. field environmental real-time detection, field germ analysis and supporting medical science. One of our setup's prominent merits is the WSCIS, which can measure the real-time “illumination wavelength” for light source with narrow spectrum (e.g. laser diode, LD). Yet quasi-monochromatic LEDs have two different characteristics from LDs. One is they have wide spectra (FWHMs in this manuscript: 15 nm~38 nm). The other is that the peak wavelength of LEDs will shift (up to 16 nm in red LEDs) due to the changes of LED input battery voltage, working current and junction temperature [22,23]. Although the wavelength shift can be prevented by current driver, cooling module and super-narrow spectral filter, their cost [24], especially multiplied by the total number of LEDs (seven in this manuscript), is further expensive than LED itself (~0.5 RMB, or 0.08 USD). Now, instead of preventing wavelength shift, our WSCIS gives a real-time computationally optimized wavelength value (COWV). The COWV is sometimes not exactly equal to the real-time peak wavelength, but it's the “best” value chosen by the wavelength-autofocusing algorithm.

The manuscript is mainly divided into the following sections: firstly, principles of holographic wavelength-autofocusing, WSCIS and portable MSLLM are presented. Secondly, the design and whole configurations will be illustrated. Thirdly, experiments about WSCIS, and an experimental example to acquire multi-spectral images of the bio-sample are presented. Fourthly, limitations and extensions of our lens-less microscope are discussed. Finally, the conclusion is drawn.

2. Principles

2.1. Holographic wavelength-autofocusing and WSCIS

As shown in Fig. 1, when an object is illuminated by a plane optical wave, the complex field on the detected plane at the distance of z is given by a convolution form:

$$U(x, y; z) = \iint U(x_0, y_0; 0) h(x - x_0, y - y_0; z) dx_0, \quad (1)$$

where, $h(x-x_0, y-y_0; z)$ is the Fresnel propagation kernel. In the Angular Spectrum theory [21], this convolution can be rewritten as:

$$A(f_x, f_y) = A_0(f_x, f_y) \cdot H(f_x, f_y), \quad (2)$$

where, f_x and f_y are Fourier frequencies in x and y directions, respectively. $A(f_x, f_y)$ and $A(f_x, f_y)$ are angular spectra of $U(x, y; z)$ and $U(x_0, y_0; 0)$ in the Fourier domain, respectively. The transfer function $H(f_x, f_y)$ can be expressed as:

$$H(f_x, f_y) = \begin{cases} \exp\left[jkz\sqrt{1 - (\lambda f_x)^2 - (\lambda f_y)^2}\right], & \sqrt{f_x^2 + f_y^2} \leq f_{\text{cut-off}}, \\ 0, & \text{others} \end{cases}, \quad (3)$$

where, $k = 2\pi/\lambda$, $\lambda = \lambda_0/n$, λ_0 is the wavelength in free space. $f_{\text{cut-off}}$ is usually determined by the pixel size of CMOS image sensor. Thus, in the Fresnel propagation [21], Eq. (1) can be also written as:

$$U(x, y; z) = FT^{-1}\{FT\{U(x_0, y_0; 0)\}H(f_x, f_y)\}, \quad (4)$$

where FT means Fourier transform, and FT^{-1} means inverse Fourier transform.

According to Eqs. (3) and (4), the Fresnel propagation transfer function is related with the refractive index n in the propagating space, the wavelength λ , and the distance between the object and the CMOS image sensor z . In the experiments, rulers cannot be used to accurately determine the diffraction distance z , which is very important in the above equations. Up to now, many distance-autofocus functions and criterions have been developed. When n and λ are the known variables, the process to determine z based on the criterions is called “distance-autofocus algorithms”, which is well-known in computational holography [25,26]. In this manuscript, a kind of edge sparsity criterion [25,26] is adopted, which is named as “Gini of Gradients” (GoG) and defined as:

$$\text{GoG}(U) = \text{Gini}(|\nabla U|), \quad (5)$$

where, ∇ is the gradient operator, $|\bullet|$ is the modulus operator, U is the reconstructed complex field, and $\text{Gini}(\bullet)$ is defined as:

$$\text{Gini}(C) = 1 - 2 \sum_{k=1}^N \frac{a[k]}{\text{sum}(C)} \left(\frac{N - k + 0.5}{N} \right), \quad (6)$$

where, $a[k]$ is the k th sorted entry of the matrix C , in the ascending order, $k = 1, \dots, N$, and $\text{sum}(C)$ is the sum of all elements in the matrix C .

From another aspect, when the variables n and z in the Fresnel propagation transfer function are known, the process based on above autofocus criterions can be used to determine λ , which we call it as “holographic wavelength-autofocus algorithms”. The procedure is: firstly, set an initial estimation range of λ , e.g. (400 nm~700 nm). Secondly, each value of λ picked by the golden-section method is input into the back-propagation algorithms based on Eqs. (3) and (4), and λ -dependent GoG value of the back-propagated hologram are calculated. Finally, according to series of the values of λ -dependent GoG, λ can be determined.

Fig. 2 presents the principle about how to calibrate an illumination wavelength by WSCIS. In Fig. 2(a), the positive pattern is illuminated by an unknown-wavelength monochromatic plane wave, whose wavelength is assumed as λ . The CMOS image sensor is parallel to the positive pattern, and the gap between them is d_0 . There are two steps to determine λ . Firstly, a known-wavelength (λ_0) (e.g. He-Ne laser) monochromatic plane wave is used to illuminate the positive pattern, as the same schematic in Fig. 2(a); a hologram, named as H_0 , is recorded by the CMOS image sensor. Based on λ_0 and H_0 , the gap d_0 can be calculated by scalar wave propagation theorem and the distance-autofocusing algorithm. Secondly, moving away the known-wavelength light source, the unknown-wavelength (λ) monochromatic plane wave is used to illuminate the positive pattern; a hologram, named as H_1 , is recorded. Based on d_0 and H_1 , the unknown-wavelength λ can be calculated by scalar wave propagation theorem and the wavelength-autofocusing algorithm.

2.2. Multi-spectral lens-less imaging

One application of our setup is to achieve multi-spectral lens-less imaging, as shown in Fig. 3. The left 1/4 part of the CMOS image sensor is faced to a fixed positive pattern, which serves as a WSCIS. The distance

Download English Version:

<https://daneshyari.com/en/article/7131199>

Download Persian Version:

<https://daneshyari.com/article/7131199>

[Daneshyari.com](https://daneshyari.com)